

Investigation of 3-D coherent structures in the turbulent cylinder wake using Tomo-PIV

F. Scarano¹, G. E. Elsinga¹, E. Bocci², B. W. van Oudheusden¹

1: Aerospace Eng. Dept., Delft University of Technology, Delft, The Netherlands, f.scarano@lr.tudelft.nl

2: Mechanics and Aeronautics Dept., Università degli Studi di Roma "La Sapienza", Rome, Italy

Keywords: Cylinder wake, Tomographic PIV, turbulence, coherent structures

The wake of a circular cylinder at $Re = 2700$ is investigated by means of Tomographic PIV (Tomo-PIV), a recently developed three-dimensional velocimetry technique (Elsinga *et al.* 2005). Experiments are performed in the open-test section of a 40x40 cm² wind tunnel with a free-stream velocity of 5 m/s and a cylinder diameter $D = 8$ mm ($Re_D = 2700$). The study focuses on the instantaneous three-dimensional structure of the wake composed of Kármán rollers and span wise distributed secondary vortices. The measurement volume extends approximately over a region of 40(H)x40(L)x10(W) mm³ with the shortest dimension in the direction of the depth of field. Two configurations are chosen in order to describe both the 2D wake features and the span wise organization of secondary rollers dominating the 3D flow organization. The Tomo-PIV technique makes use of 4 CCD cameras observing simultaneously the light scattered by the particle tracers within a 3D domain from different directions covering a solid angle. The reconstruction of the 3D particle field from its projections is performed with an adapted MART algorithm for PIV images and the resulting objects are interrogated with 3D cross-correlation software following the iterative multi-grid approach. The velocity field is returned on a grid of 64x64x30 vectors. The present data allow to directly evaluate the measurement error imposing mass conservation inside the volume (viz. solenoidal velocity field). The visualization of the wake instantaneous structure is obtained by means of vorticity vector magnitude iso-surfaces, or decomposing the vorticity along the span wise and stream-wise/vertical component respectively. This allows to distinguish between the contribution of the Kármán rollers and the interconnecting structures between them respectively. The transverse view of the wake (figure 1-right) shows the shear layers separating from the cylinder surface as vorticity sheets rolling up downstream during the formation of Kármán vortices. The fluctuations within the main rollers are ascribed to the transition of the free shear layers which leads to the formation of discrete vortices subsequently rolling-up in a single structure. The vorticity stretching activity is observed to peak in the stream wise structures. The three-dimensional pattern of the vorticity vector in the span wise view of the wake (figure 2) is represented plotting iso-surfaces of the span wise component (green for $\omega_y = 2 \times 10^3$ s⁻¹, cyan for $\omega_y = -2 \times 10^3$ s⁻¹) and of the combination of the normal and bi-normal components (red for $\omega_{xz} = 2 \times 10^3$ s⁻¹, blue for $\omega_{xz} = -2 \times 10^3$ s⁻¹). The primary rollers appear well correlated along the span in the vicinity of the cylinder $X/D = 1$, although undulated under the effect of the stream wise vortices pairs. They undergo further three-dimensional distortion downstream of $X/D = 3$. Peak vorticity levels of 5×10^3 s⁻¹ are observed for the primary rollers during the formation

process which agrees with literature data from planar PIV (Huang *et al.* 2006), decaying slowly (only 25% decay at $X/D = 3$) downstream. The secondary rollers are organized as pairs of counter-rotating stream wise and vertically oriented structures interconnecting the primary rollers similarly to the instability *Mode B* occurring in lower Reynolds number wakes investigated with previous studies (Williamson, 1996). A value of the span wise wavelength $\lambda_z/D = 1.2$ is inferred from the instantaneous visualizations and confirmed by a statistical analysis performed with the autocorrelation of vorticity-indicator function. The pattern of vorticity for the secondary rollers shows counter-rotating vortex pairs (red-blue) developed in the braid shear layer region and interconnecting the two primary rollers close to the cylinder.

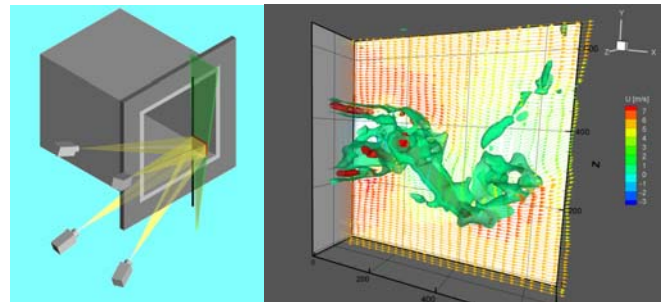


Fig. 1 – Left: schematic of illumination and imaging for Tomo-PIV. Right a sample 3D instantaneous velocity vector field and vorticity iso-surfaces

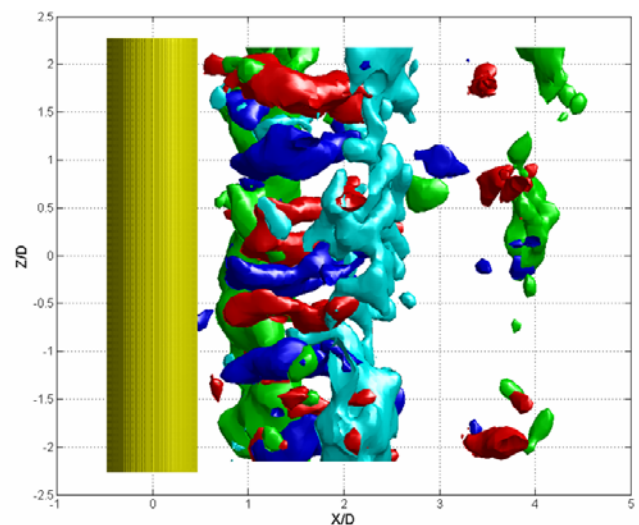


Fig. 2 – Instantaneous vorticity iso-surfaces ($atw = 2 \times 10^3$ s⁻¹).
Color coding: $\omega_z > 0$ green; $\omega_z < 0$ cyan;
 $\sqrt{\omega_x^2 + \omega_y^2} \cdot \text{sign}(\omega_x) > 0$ red; $\sqrt{\omega_x^2 + \omega_y^2} \cdot \text{sign}(\omega_x) < 0$ blue.